

# Alpha decay and nuclear deformation: the case for favoured alpha transitions of even-even emitters

*F. García\* and O. Rodríguez†*

Instituto de Física, Universidade de São Paulo,  
Caixa Postal 66318, 05315-970, São Paulo-SP, Brasil.

*M. Gonçalves*

Instituto de Radioproteção e Dosimetria — IRD/CNEN,  
Av. Salvador Allende s/n, 22780-160 Rio de Janeiro-RJ, Brasil.

*S. B. Duarte‡, O. A. P. Tavares, and F. Guzmán†*

Centro Brasileiro de Pesquisas Físicas — CBPF/CNPq,  
Rua Dr. Xavier Sigaud 150, 22290-180 Rio de Janeiro-RJ, Brasil.

Alpha-decay half-life for ground-state to ground-state transitions of 174 even-even alpha emitters has been calculated from a simple, Gamow-like model in which the quadrupole deformation of the product nucleus (assumed to have an ellipsoidal shape) is taken into account. The assumption made is that before tunnelling through a purely Coulomb potential barrier the two-body system oscillates isotropically, thus giving rise to an equivalent, average polar direction  $\theta_0$  (referred to the symmetry axis of the ellipsoid) for alpha emission. It is shown that the experimental half-life data are much better reproduced by the present description than in the spherical-shaped approximation for the daughter nucleus.

PACS: 23.60.+e

---

\*Permanent address: Departamento de Ciências Exatas e Tecnológicas, Universidade Estadual de Santa Cruz, 45650-000, Ilhéus-Ba, Brasil.

†Permanent address: Instituto Superior de Ciencias y Tecnologia Nucleares, Av. Salvador Allende y Luaces, Apartado Postal 6163, La Habana, Cuba.

‡Electronic address: sbd@cbpf.br.

## I. INTRODUCTION

The alpha-decay process in axially deformed nuclei has been studied by various authors. Berggren [1] has calculated half-lives and anisotropies in the alpha decay for a number of axially symmetric deformed nuclei. A microscopic description of the alpha decay of deformed nuclei has been developed in recent years by Delion *et al.* [2–5], who have treated the alpha-decay process in two steps, namely, *i*) the behaviour of the four nucleons to constitute the alpha particle by their clustering on the nuclear surface, and *ii*) the penetration of the alpha particle through the Coulomb barrier by using the classical WKB approximation [6]. In addition, an exact description of the process of penetration through a deformed barrier as well as the influence of the deformation on both the formation amplitude and penetrability have been discussed very recently by Delion and Liotta [7]. Also, Stewart *et al.* [8] have found that it is possible to describe all known branching ratios of even-even actinide nuclei with a practically nucleus-independent alpha-particle wave function near the nuclear surface. The constant internal amplitudes give good results to the observed anisotropies in the favoured alpha decay of four odd-even deformed actinide nuclei as reported in [8]. From the experimental point of view, a number of important observations of remarkably pronounced preferential alpha emission in oriented odd-*A* alpha emitters have been reported by Hanauer *et al.* [9], Navarro *et al.* [10], Soinski *et al.* [11], Dilmanian *et al.* [12], and more recently by Soinski and Shirley [13], Wouters *et al.* [14], and Schuurmans *et al.* [15]. This latter work showed for the first time that anisotropic alpha emission in favoured decays is mainly determined by the structure (shell effects) of the decaying nucleus, being not necessarily related to deformation.

Even-even product nuclei from ground-state to ground-state alpha decay exhibit, except for a few cases, some degree of nuclear deformation [16–18]. The effect of quadrupole deformation of the product nucleus on the estimated half-life for favoured alpha transitions of even-even nuclei has been discussed alternatively in [19] by means of a simple, Gamow-like model, which yields a formula with no adjustable parameter to calculate the alpha-decay half-life. This formalism has been successfully applied to some cases of preferred alpha decay of even-even nuclei ( $^{252}\text{Cf} \rightarrow ^{248}\text{Cm}$ ,  $^{190}\text{Pt} \rightarrow ^{186}\text{Os}$ , and  $^{184}\text{Pb} \rightarrow ^{180}\text{Hg}$ ), for which cases the daughter nucleus exhibit essentially a quadrupole deformation.

Results have shown that the predicted half-life values agree with the measured ones much better than in the spherical-shaped approximation for the product nucleus. The examples reported showed that little changes from the spherical to either prolate and oblate shape of the product nucleus led to the emission of the alpha particle at a certain equivalent, average polar direction  $\theta_0$  (referred to the symmetry axis of the ellipsoidal shape of the product nucleus) for the preferred alpha transitions mentioned above [19].

Since then, the expectation has been that the experimental half-lives of all cases of preferred alpha emissions which produce even-even deformed nuclei should be better reproduced when deformation is taken into account in Gamow-like model than in its spherical approximation. The present paper reports, therefore, on a systematic half-life prediction study over 174 cases of preferred alpha transitions of measured half-lives available in the literature. Comparison between the present systematics and previous studies [20–22] is also briefly reported.

## II. MODEL ASSUMPTIONS

The main assumptions of the referenced model are here summarized. (i) The shape of the product nucleus is supposed to be the one of an ellipsoid of revolution with semi-axes  $a = b \neq c$ , the amount of deformation,  $d = 250Q_2/Z_2$ , being defined by the nuclear intrinsic electric quadrupole moment,  $Q_2$  (in barn), of the ground-state product nucleus ( $Z_2$  is its atomic number, and  $d$  is in  $\text{fm}^2$ ). (ii) The  $Q_\alpha$ -value as well as the reduced mass,  $\mu$ , of the disintegrating system are calculated from the nuclear (rather than the atomic) mass values of the participating nuclides. (iii) The frequency of oscillation for the relative two-body motion ( $\lambda_0 \approx 10^{21} \text{ s}^{-1}$ ) is calculated as

$$\lambda_0(\theta, d) = \frac{v}{2s_0(\theta, d)}, \quad (1)$$

where  $\theta$  is the polar angle referred to the symmetry axis of the ellipsoid,  $v = (2Q_\alpha/\mu)^{1/2}$  is the relative velocity, and  $s_0$  denotes the separation between the centres of the fragments at contact. This latter quantity is given by

$$s_0(\theta, d) = \frac{1}{[A - (A - C) \cos^2 \theta]^{1/2}}, \quad (2)$$

where

$$A = (a + R_\alpha)^{-2}, \quad \text{and} \quad C = (c + R_\alpha)^{-2}. \quad (3)$$

(iv) The value for the equivalent sharp charge radius of the alpha particle,  $R_\alpha$ , is set equal to  $(1.62 \pm 0.01)$  fm, as it comes from the charge density distribution resulting from data on elastic electron scattering from  $^4\text{He}$  as obtained by Sick *et al.* [23]. (v) The configuration at contact is defined at the sharp surface of the neutron (rather than the charge) density distribution of the product nucleus; the semi-axes of the ellipsoidal shape of the product nucleus are determined by assuming that the neutron density distribution deforms in the same way as the charge density distribution does, where volume is preserved in both cases; accordingly, the semi-axes are calculated by

$$a = b = \sqrt{R_{n_2}^3/c}, \quad \text{and} \quad c = 2^{-1/3}R_{n_2}[(1+B)^{1/3} + (1-B)^{1/3}], \quad (4)$$

where

$$B = \left[ 1 - 4 \left( \frac{d}{3R_{ch_2}^2} \right)^3 \right]^{1/2}, \quad (5)$$

and  $R_{n_2}$  and  $R_{ch_2}$  are the equivalent sharp radius of the neutron and charge distribution, respectively, of the product nucleus. (vi) Before tunnelling through the potential barrier the two-body system oscillates isotropically, giving rise to an average frequency of oscillation,  $\bar{\lambda}_0(d)$ , which corresponds to an equivalent, average value for the polar direction  $\theta_0$  of alpha emission; this assumption is expressed by

$$\bar{\lambda}_0(d) = \frac{1}{4\pi} \int_0^\pi \lambda_0(\theta, d) 2\pi \sin \theta d\theta = \lambda_0(\theta_0, d), \quad (6)$$

which leads to an alpha-particle emission at an equivalent, average polar direction  $\theta_0$ .

(vii) The decay constant

$$\lambda(d) = \bar{\lambda}_0(d)P(d, \theta_0) \quad (7)$$

is therefore calculated at such average  $\theta_0$ -value, where

$$P(d, \theta_0) = \exp[-G(d, \theta_0)] \quad (8)$$

is the penetrability factor through a purely Coulomb potential barrier,  $V(d, \theta_0, s)$ , at separation  $s \geq s_0(d, \theta_0)$ , and  $G(d, \theta_0)$  is Gamow's factor for decay; this latter quantity is given by the classical WKB-integral approximation.

Accordingly, equations (1)–(3) and (6) are handled to give

$$\cos \theta_0 = \left\{ \left(1 - \frac{C}{A}\right)^{-1} - \left[ \frac{1}{2} \left( \left(\frac{A}{C} - 1\right)^{-1/2} + \left(1 - \frac{C}{A}\right)^{-1} \times \arcsin \left(1 - \frac{C}{A}\right)^{1/2} \right) \right]^2 \right\}^{1/2}, \quad (9)$$

which is valid for prolate-shaped product nuclei, i.e.,  $Q_2 > 0$ ,  $a < c$ , and  $C/A < 1$ , and

$$\cos \theta_0 = \left\{ \left[ \frac{1}{2} \left( \left(1 - \frac{A}{C}\right)^{-1/2} + \left(\frac{C}{A} - 1\right)^{-1} \times \operatorname{arcsinh} \left(\frac{C}{A} - 1\right)^{1/2} \right) \right]^2 - \left(\frac{C}{A} - 1\right)^{-1} \right\}^{1/2}, \quad (10)$$

which is valid for oblate-shaped product nuclei, i.e.,  $Q_2 < 0$ ,  $a > c$ , and  $C/A > 1$ .

It results that the equivalent, average polar direction for alpha emission is found to vary very weakly within the range of deformation of known even-even nuclei [16,17]. As a matter of fact, from equations (9) and (10) the values of  $\theta_0$  have been calculated to give  $\sim 53.4$ – $54.7$  degree for prolate cases, and  $\sim 54.8$ – $56.0$  degree for the oblate-shaped nuclei.

### III. ROUTINE CALCULATION FOR ALPHA-DECAY HALF-LIFE

From assumptions (i)–(vii) above, and by expressing masses in u, energies in MeV, lengths in fm, and time in second, the following formula emerges to calculate the alpha-decay half-life:

$$\tau_c = 1.0 \times 10^{-22} \left( \frac{\mu}{Q_\alpha} \right)^{1/2} s_0(d, \theta_0) \exp \left[ 0.5249578932 (Z_1 Z_2 \mu)^{1/2} I \right], \quad (11)$$

where

$$I = \int_{s_0}^{s'} \left[ \frac{g(d, \theta_0, s)}{s} - q \right]^{1/2} ds, \quad \text{and} \quad q = \frac{Q_\alpha}{Z_1 Z_2 e^2}, \quad (12)$$

$Z_1 = 2$ ,  $e^2 = 1.4399652$  MeV.fm is the square of the electronic elementary charge, and  $s'$  (the outer turning point in the WKB-integral) is the solution of the equation  $g(d, \theta_0, s') =$

$qs'$ . The quantity  $g(d, \theta_0, s)$  gives the contribution to the Coulomb potential energy,  $V(d, \theta_0, s) = Z_1 Z_2 e^2 g(d, \theta_0, s)/s$ , due to the interaction between the alpha particle and the prolate- or oblate-shaped (only quadrupole deformation) product nucleus at  $s \geq s_0$ , and it has been deduced as

$$g(d, \theta_0, s) = \frac{3}{2} \left\{ \frac{n}{(x)^{1/2}} \operatorname{arcsinh} \left[ (x)^{1/2} \left( \frac{2}{m-x} \right)^{1/2} \right] + p \right\} \quad (13)$$

for prolate deformation ( $Q_2 > 0$ ,  $d > 0$ ,  $x = d/s^2 > 0$ ), and

$$g(d, \theta_0, s) = \frac{3}{2} \left\{ \frac{n}{(-x)^{1/2}} \operatorname{arcsin} \left[ \sqrt{-x} \left( \frac{2}{m-x} \right)^{1/2} \right] + p \right\} \quad (13')$$

for oblate deformation ( $Q_2 < 0$ ,  $d < 0$ ,  $x = d/s^2 < 0$ ), where the quantities  $m$ ,  $n$ , and  $p$  are given by

$$m = 1 + (1 - 2x \cos 2\theta_0 + x^2)^{1/2}, \quad (14)$$

$$n = 1 + \frac{1 - 3 \cos^2 \theta_0}{2x}, \quad (15)$$

$$p = \frac{(2)^{1/2} \cos^2 \theta_0}{x(m+x)^{1/2}} - \frac{(m+x)^{1/2} \sin^2 \theta_0}{(2)^{1/2} x(m-x)}. \quad (16)$$

If one assumes the product nucleus having the spherical shape, then  $Q_2 = 0$ ,  $d = 0$ ,  $a = b = c = R_{n_2}$ ,  $s_0 = R_{n_2} + R_\alpha$ ,  $V(s) = Z_1 Z_2 e^2/s$ , and  $s' = 1/q$ , and, therefore, the predicted alpha-decay half-life according to the present Gamow-like model turns out to be given by the usual expression

$$\tau_c = 1.0 \times 10^{-22} \left( \frac{\mu}{Q_\alpha} \right)^{1/2} s_0 \exp(G), \quad (17)$$

$$G = 0.629941859 Z_1 Z_2 \left( \frac{\mu}{Q_\alpha} \right)^{1/2} \{ \arccos \sqrt{qs_0} - [qs_0(1 - qs_0)]^{1/2} \}. \quad (18)$$

#### IV. INPUT DATA

According to assumption (ii) above (section 2) the  $\mu$ - and  $Q_\alpha$ -values are calculated from the expressions

$$Q_\alpha = [(\Delta M)_p - (\Delta M)_2] + 10^{-6} \times [kZ_p^\ell - kZ_2^\ell] - 2.424989456 \text{ MeV}, \quad (19)$$

$$\frac{1}{\mu} = \frac{1}{m_2} + \frac{1}{m_\alpha}, \quad (20)$$

$$m_2 = A_2 + \frac{(\Delta M)_2}{F} - Z_2 m_e + \frac{10^{-6}}{F} \times kZ_2^\ell \text{ u}, \quad (21)$$

where  $m_2$  is the nuclear mass of the daughter nucleus,  $m_\alpha = 4.0015061747 \text{ u}$  is the alpha-particle mass [24],  $m_e = 548579903 \times 10^{-12} \text{ u}$  is the electron rest mass [24],  $F = 931.49386 \text{ MeV/u}$  is the mass-energy conversion factor [25], and the  $\Delta M$ 's are the atomic mass-excess-values taken from the 1995 Mass Table by Audi and Wapstra [25], except for the alpha decay of  $^{166}\text{Pt}$ ,  $^{174}\text{Hg}$ ,  $^{180}\text{Pb}$ , and  $^{202}\text{Ra}$  parent nuclei and their respective daughter nuclei, for which cases the  $\Delta M$ -values are those tabulated in [17]. The quantity  $kZ^\ell$  represents the total binding energy of the  $Z$  electrons in the atom, where the values for the constants  $k$  and  $\ell$  have been derived from data reported by Huang *et al.* [26], thus obtaining

$$\begin{cases} k = 8.7 \text{ eV} \\ \ell = 2.517 \end{cases} \quad \text{for } Z \geq 60, \quad (22)$$

and

$$\begin{cases} k = 13.6 \text{ eV} \\ \ell = 2.408 \end{cases} \quad \text{for } Z < 60. \quad (23)$$

The values for the intrinsic electric quadrupole moment of the ground-state daughter nucleus,  $Q_2$  (in barn), have been taken as the average of three different  $Q_2$  evaluations. The first one comes from the routine calculation developed in the framework of the nuclear droplet model updated by Myers and Schmidt [27],

$$Q_2 \simeq \frac{3}{500} Z_2 R_{ch_2}^2 \sqrt{\frac{5}{\pi}} \beta_2 \left( 1 + \frac{2}{7} \sqrt{\frac{5}{\pi}} \beta_2 \right), \quad (24)$$

where  $R_{ch_2}$  is the equivalent sharp radius of the charge distribution (see below), and  $\beta_2$  is the ground-state quadrupole deformation parameter, the values of which have been taken from the recent tabulation by Möller *et al.* [17]. The second and third sources of  $Q_2$ -data are a previous tabulation of the  $Q_2$ -values calculated with a macroscopic-microscopic nuclear model by Möller and Nix [16], and the compilation of calculated and

experimental  $Q_2$ -values reported by Nerlo-Pomorska and Mach [18]. It results that the maximum uncertainty in the averaged  $Q_2$ -values is about 15%.

The  $R_{ch_2}$ -values have been evaluated from the average  $r_{ch} = \overline{\langle r_{ch_2}^2 \rangle}^{1/2}$  of the nuclear root-mean-square charge radius values taken from a number of compilations and systematics of charge radii [18,27–35], where the droplet model description for the radial moments has been used following Myers and Schmidt [27], thus obtaining

$$R_{ch_2} = \frac{1}{2} \left\{ \left( 4.41 \times 10^{-6} Z_2^2 + \frac{20}{3} \times r_{ch}^2 - 19.602 \right)^{1/2} - 2.1 \times 10^{-3} Z_2 \right\}. \quad (25)$$

The values for the equivalent sharp radius of the neutron density distribution of the product nucleus,  $R_{n_2}$ , are taken as the average of two equivalent sharp neutron radius evaluations as already detailed in [19]. The former is given by the tabulated neutron sharp radius values following the droplet model description of atomic nuclei [36], and the latter comes from the most recent systematics of root-mean-square neutron radii in even-even nuclei by Dobaczewski *et al.* [35].

Finally, the experimental alpha-decay half-life values,  $\tau_e$ , have been updated from the most recent edition produced by the NNDC (BNL, Upton, N.Y., USA) [37], and the latest issues of the Nuclear Data Sheets [38] (for  $^{190}\text{Pt}$  we have used the recent experimental value quoted in [39]). Accordingly, we have collected a total of 165 cases of ground-state to ground-state alpha decay of even-even parent nuclei of known  $\tau_e$ , plus 9 cases of limiting  $\tau_e$ -values. We noticed 128 cases involving prolate daughter nuclei, 32 oblate ones, and 14 cases leading to spherical daughter nucleus.

The degree of deformation of the nuclei considered in the present study, here defined by the dimensionless quantity

$$\delta = \frac{100Q_2}{Z_2 R_{ch_2}^2}, \quad (26)$$

can be appreciated in Fig. 1, which reveals a tendency towards sphericity for nuclei near the 82 and 126 neutron shell closure. Figure 2 shows the behaviour of the reduced, equivalent sharp charge (Fig. 2-a) and neutron (Fig. 2-b) radii with daughter nucleus mass number. It is seen that the relative broad minima in Fig. 2-b and the corresponding relative broad maxima in Fig. 2-a indicate the regions of mass of the highly neutron-deficient alpha emitters, viz.,  $A_p \approx 100$  and  $150 \lesssim A_p \lesssim 170$ . In addition, a number

of proton-deficient alpha emitters is seen in Fig. 2 to be located in the mass range  $200 \lesssim A_p \lesssim 230$ . For nuclei of  $A_2 \gtrsim 140$  the reduced neutron radii result  $\sim 1\text{--}4\%$  greater than the reduced charge radii; on the contrary, in the region of  $A_2 \approx 100$  the reduced charge radii are  $\sim 1\%$  greater than the neutron radii.

## V. RESULTS AND DISCUSSION

The preferred alpha decay of  $^{252}\text{Cf}$  and  $^{190}\text{Pt}$  isotopes have been selected to test the present model (Fig. 3). The corresponding prolate product nuclei,  $^{248}\text{Cm}$  and  $^{186}\text{Os}$ , exhibit essentially a quadrupole deformation ( $Q_2 = 12$  b and 5.4 b, respectively). The predicted alpha-decay half-lives result to be  $0.82 \times 10^8$  s for  $^{252}\text{Cf}$ , and  $0.93 \times 10^{19}$  s for  $^{190}\text{Pt}$ , which values are in very good agreement with the experimental ones ( $1.0 \times 10^8$  s and  $1.0 \times 10^{19}$  s, respectively). The variation of calculated half-life,  $\tau_c$ , with intrinsic electric quadrupole moment of the product nucleus,  $Q_2$ , is shown in Fig. 3 for the examples reported above. The trend is a monotonous increase of  $\tau_c$  with increasing  $Q_2$ , in such a way that the half-life-values calculated under the assumption of spherical-shaped ( $Q_2 = 0$ ) product nucleus result more distant from the experimental one than those estimated when quadrupole deformation of the product nucleus is taken into account. The same happens to cases of oblate product nuclei, of which two examples ( $^{192}\text{Pb}$  and  $^{204}\text{Ra}$  alpha emitters) are depicted in Fig. 4. Again, the effect of quadrupole deformation of the product nucleus is to increase the estimated half-life-value from the one obtained when the spherical-shaped approximation is used. The effect of deformation on the predicted half-lives results to be small. Calculations have indicated that, depending on the amount of the quadrupolar deformation, the predicted alpha-decay half-life is 3–43% larger than that obtained under the spherical-shaped approximation for the daughter nucleus (see Fig. 6-b bellow).

A systematic alpha-decay half-life prediction study has been carried out within the framework of the present Gamow-like model, where calculated values have been compared with available experimental data [37–39]. Results are summarized in Table I, where the values of the main quantities related to various distributions of the ratio  $q = \log_{10}(\tau_c/\tau_e)$  are listed to allow a comparison between each other. Inspection on Table I allows one to conclude that: (i) the experimental half-lives of preferred alpha transitions producing

deformed (either prolate or oblate) nuclei are better reproduced when quadrupole deformation of the daughter nucleus is taken into account in Gamow-like model than in the spherical approximation ( $Q_2 = 0$ ). This result is valid for the sub-set of cases leading to daughter nuclei actually deformed to some extent ( $|\delta| > 0.05$ , columns 5 and 7 of Table I). When all data are considered the difference between the two approaches is not evident in view of the presence of 63 cases of spherical plus quasi-spherical product nuclei. Anyway, all  $q$ -distributions show to be centred around the mean value  $\bar{q} \approx 0$ , and the statistics is better than, or comparable to, other systematics reported in Table I (columns 2, 3, and 4). Figure 5 shows the frequency distributions of  $q = \log_{10}(\tau_c/\tau_e)$  for the sub-set of cases of  $|\delta| > 0.05$ . These distributions are seen normal-like ones. (ii) The predictive power of alpha-decay half-life following the present formalism is as much the same as, or better than, the referenced previous alpha decay systematics carried out with two [20,22] or four [21] model parameters. We remark that the present Gamow-like formalisms (ellipsoidal- and spherical-shaped product nucleus approximations) do not contain any adjustable model parameter. Figure 6 shows the comparison between calculated ( $\tau_c$ ) and experimental ( $\tau_e$ ) alpha decay half-life-values for a total of 166 cases of known  $\tau_e$  for the deformed approximation of the product nucleus (Fig. 6-a). It is estimated that  $\sim 90\%$  of the half-life data are predicted within a factor of 4 when the ellipsoidal shape of the product nucleus has been considered in the calculation. The effect of deformation on the calculated half-lives can be appreciated in Fig. 6-b. Finally, Table II compares the predicted half-life-values following both shape descriptions for the product nucleus with experimental values compiled from Refs. [37–39].

## VI. CONCLUSION AND FINAL REMARKS

In the present work a simple, Gamow-like model for alpha decay which takes into account the quadrupole deformation of the product nucleus has been developed to systematize 174 half-life-values of preferred alpha transitions of even-even emitters. The  $Q$ -value for alpha decay as well as the reduced mass of the disintegrating system have been obtained from nuclear (rather than atomic) mass-values deduced from updated atomic mass evaluations [24,25]. The configuration at contact of the alpha particle with the daughter

nucleus has been defined at the sharp surface of the neutron density distribution which has been supposed to deform in the same way as the charge density does. Reliable values for the equivalent sharp radii for both the charge and neutron distributions have been used throughout the half-life routine calculations. The basic assumption has been made that before tunnelling through a purely Coulomb potential barrier the disintegrating system oscillates isotropically to give an average frequency of oscillation  $\lambda_0$  which does correspond to an equivalent, average polar direction,  $\theta_0$  (referred to the symmetry axis of the ellipsoidal shape of the product nucleus), for alpha emission, which is expected to occur for all cases of both prolate- and oblate-shaped even-even product nucleus.

Accordingly, this simple model has shown pretty good in reproducing the available experimental alpha decay half-life data for the preferred alpha emission of even-even emitters. The predictive power of the present model is able to systematize the referred data in a way comparable with, or better than, the existing alpha-decay half-life systematics. In addition, the present formalism has been developed without any adjustable parameter. Finally, we have shown that, statistically, the experimental data for cases of daughter nuclei which exhibit quadrupole deformation (either prolate or oblate) are better reproduced by the model when the effect of deformation is taken into account than in the spherical approximation for the product nucleus.

### ACKNOWLEDGMENTS

The authors wish to express their gratitude to the Brazilian CNPq, CLAF, FAPERJ, and FAPESP for partial support.

- 
- [1] Berggren, T., Phys. Rev. C **50**, 2494 (1994). See also Berggren, T. and Olanders, P., Nucl. Phys. **A473**, 189 (1987).
- [2] Insolia, A., Curutchet, P., Liotta, R. J. and Delion, D. S., Phys. Rev. C **44**, 545 (1991).
- [3] Delion, D. S., Insolia, A. and Liotta, R. J., Phys. Rev. C **46**, 1346 (1992).
- [4] Delion, D. S., Insolia, A. and Liotta, R. J., Phys. Rev. C **46**, 884 (1992).
- [5] Lovas, R. G., Liotta, R. J., Insolia, A., Varga, K. and Delion, D. S., Phys. Rep. **294**, 265 (1998).
- [6] Fröman, P. O., Mat. Fys. Skr. Dan. Vid. Selsk. **1**, No. 3 (1957); Bohr, A., Fröman, P. O. and Mottelson, B., Dan. Mat. Fys. Medd. **29**, No. 10 (1955).
- [7] Delion, D. S., and Liotta, R. J., Phys. Rev. C **58**, 2073 (1998).
- [8] Stewart, T. L., Kermode, M. W., Beachey, D. J., Rowley, N., Grant, I. S. and Kruppa, A. T., Phys. Rev. Lett. **77**, 36 (1996).
- [9] Hanauer, S. H., Dabbs, J. W. T., Roberts, L. D. and Parker, G. W., Phys. Rev. **124**, 1512 (1961).
- [10] Navarro, Q. O., Rasmussen, J. O. and Shirley, D. A., Phys. Lett. **2**, 353 (1962).
- [11] Soinski, A. J., Frankel, R. B., Navarro, Q. O. and Shirley, D. A., Phys. Rev. C **2**, 2379 (1970).
- [12] Dilmanian, F. A., Sarantites, D. G., Jääskeläinen, M., Puchta, H., Woodward, R., Beene, J. R., Hensley, D. C., Halbert, M. L., Novotny, R., Adler, L., Choudhury, R. K., Namboodiri, M. N., Schmitt, R. P. and Natowitz, J. B., Phys. Rev. Lett. **49**, 1909 (1982).
- [13] Soinski, A. J. and Shirley, D. A., Phys. Rev. C **10**, 1488 (1974).
- [14] Wouters, J., Vandeplassche, D., Van Walle, E., Severijns, N. and Vanneste, L., Phys. Rev. Lett. **56**, 1901 (1986).

- [15] Schuurmans, P., Will, B., Berkes, I., Camps, J., De Jesus, M., De Moor, P., Herzog, P., Lindroos, M., Paulsen, R., Severijns, N., Van Geert, A., Van Duppen, P., Vanneste, L. and NICOLE and ISOLDE Collaborations, *Phys. Rev. Lett.* **77**, 4720 (1996).
- [16] Möller, P. and Nix, J. R., *At. Data Nucl. Data Tables* **26**, 165 (1981).
- [17] Möller, P., Nix, J. R., Myers, W. D. and Swiatecki, W. J., *At. Data Nucl. Data Tables* **59**, 185 (1995).
- [18] Nerlo-Pomorska, B. and Mach, B., *At. Data Nucl. Data Tables* **60**, 287 (1995).
- [19] Tavares, O. A. P., *Nuovo Cimento* **110A**, 497 (1997).
- [20] Brown, B. A., *Phys. Rev. C* **46**, 811 (1992).
- [21] Buck, B., Merchant, A. C. and Perez, S. M., *At. Data Nucl. Data Tables* **54**, 53 (1993).
- [22] Tavares, O. A. P., Duarte, S. B., Rodríguez, O., Guzmán, F., Gonçalves, M. and García, F., *J. Phys. G: Nucl. Part. Phys.* **24**, 1757 (1998).
- [23] Sick, I., McCarthy, J. S. and Whitney, R. R., *Phys. Lett.* **B64**, 33 (1976).
- [24] Audi, G. and Wapstra, A. H., *Nucl. Phys.* **A565**, 1 (1993).
- [25] Audi, G. and Wapstra, A. H., *Nucl. Phys.* **A595**, 409 (1995).
- [26] Huang, K. -N., Aoyagi, M., Chen, M. H., Crasemann, B. and Mark, H., *At. Data Nucl. Data Tables* **18**, 243 (1976).
- [27] Myers, W. D. and Schmidt, K. -H., *Nucl. Phys.* **A410**, 61 (1983).
- [28] Brown, B. A., Bronk, C. R. and Hodgson, P. E., *J. Phys. G* **10**, 1683 (1984).
- [29] Wesolowski, E., *J. Phys. G* **10**, 321 (1984).
- [30] De Vries, H., De Jager, C. W. and De Vries, C., *At. Data Nucl. Data Tables* **36**, 495 (1987).
- [31] Nadjakov, E. G., Marinova, K. P. and Gangrsky, Yu. P., *At. Data Nucl. Data Tables* **56**, 133 (1994).
- [32] Nerlo-Pomorska, B. and Pomorski, K., *Z. Phys. A* **348**, 169 (1994).

- [33] Aboussir, Y., Pearson, J. M., Dutta, A. K. and Tondeur, F., *At. Data Nucl. Data Tables* **61**, 127 (1995).
- [34] Fricke, G., Bernhardt, C., Heilig, K., Schaller, L. A., Schellenberg, L., Shera, E. B. and De Jager, C. W., *At. Data Nucl. Data Tables* **60**, 177 (1995).
- [35] Dobaczewski, J., Nazarewicz, W. and Werner, T. R., *Z. Phys.* **A354**, 27 (1996).
- [36] Myers, W. D., *Droplet Model of Atomic Nuclei* (Plenum, New York 1977).
- [37] Nuclear Data (Nudat) Retrieval Program, generated at the National Nuclear Data Center, Brookhaven National Laboratory, Upton N.Y. (USA), March 1998.
- [38] Tuli, J. K. (Editor), *Nucl. Data Sheets* **56–82** (1989–1997); *Nuclear Wallet Cards (5th Edition)*, National Nuclear Data Center, Brookhaven National Laboratory, Upton N.Y. (USA), 1995.
- [39] Tavares, O. A. P. and Terranova, M. L., *Radiat. Meas.* **27**, 19 (1997).

## FIGURE CAPTIONS

**Fig. 1:** Reduced nuclear intrinsic electric quadrupole moment,  $\delta$ , plotted against neutron number of the daughter nucleus,  $N_2$ , for 174 cases of favoured alpha transitions of even-even emitters ( $Q_2$  in barn and  $R_{ch_2}$  in fm). The lines connect data-point of a given isotopic sequence.

**Fig. 2:** Values of  $R_{ch_2}/A_2^{1/3}$  (Fig. 2-a) and  $R_{n_2}/A_2^{1/3}$  (Fig. 2-b) plotted against mass number of the daughter nucleus,  $A_2$ , for the cases of alpha decay studied in the present work; the lines connect results (points) of a given isotopic sequence.

**Fig. 3:** Variation of the calculated alpha-decay half-life,  $\tau_c$ , with nuclear intrinsic electric quadrupole moment,  $Q_2$ , for two cases of prolate product nucleus:  $^{190}\text{Pt} \rightarrow ^{186}\text{Os}$  (a), and  $^{252}\text{Cf} \rightarrow ^{248}\text{Cm}$  (b). Points indicate experimental values.

**Fig. 4:** The same as in Fig. 3, but for two cases of oblate product nucleus:  $^{192}\text{Pb} \rightarrow ^{188}\text{Hg}$  (a), and  $^{204}\text{Ra} \rightarrow ^{200}\text{Rn}$  (b).

**Fig. 5:** Frequency distribution of the quantity  $q = \log_{10}(\tau_c/\tau_e)$  for calculated alpha decay half-life-values,  $\tau_c$ , according to the present Gamow-like model: the histograms in part a) and b) refer to data listed, respectively, in columns 6 and 7 of Table II for the cases of  $|\delta| > 0.05$  (see also Table I).

**Fig. 6:** The ratio  $\tau_c/\tau_e$  (in  $\log_{10}$ -scale) of calculated to experimental alpha-decay half-life (points in part a)) is plotted against neutron number of the product nucleus,  $N_2$ ; the hatched area around the horizontal full line ( $q = 0$ ) indicates two standard deviations; it is shown results for 166 cases of alpha decay including deformation of the product nucleus following the present Gamow-like model. Part b) shows the effect of deformation on half-lives through the quantity  $q' = \log_{10}\left(\frac{\tau_d}{\tau_s}\right)$ , which is plotted against  $N_2$  ( $\tau_d$  is the calculated half-life when quadrupolar deformation is considered, and  $\tau_s$  is that value under the spherical approximation of the daughter nucleus); the lines connect data-point of a given isotopic sequence.

Table I: Standard deviation (in decimal logarithm scale),  $\sigma$ , mean value,  $\bar{q}^a$ , number of cases,  $N$ , and number of model parameters,  $n$ , for various alpha-decay half-life systematics of ground-state to ground-state transitions of even-even emitters. (For the present systematics we reject, after one run, the alpha-decay cases for which  $|q| > 2\sigma$  so as to obtain the final values listed for the quantities  $\sigma$ ,  $\bar{q}$ , and  $N$ ).

Quantity	Present Gamow-like model						
	Previous Systematics			Deformed product nucleus approx.	Spherical product nucleus approx.		
	Ref. [20]	Ref. [21]	Ref. [22]	Cases of $ \delta  > 0.05^b$	All data	Cases of $ \delta  > 0.05^b$	All data
$\sigma$	0.33	0.287	0.287	0.266	0.325	0.291	0.325
$\bar{q}$	-0.150	-0.020	0.003	0.030	0.034	-0.038	-0.020
$N$	119	147	151	95 <sup>c</sup>	157 <sup>e</sup>	97 <sup>d</sup>	156 <sup>f</sup>
$n$	2	4	2	0	0	0	0

$$^a \bar{q} = \frac{1}{N} \sum_{i=1}^N \log_{10} \left( \frac{\tau_c^i}{\tau_e^i} \right).$$

<sup>b</sup>See Fig. 1.

<sup>c</sup>Eight cases rejected in one run.

<sup>d</sup>Six cases rejected in one run.

<sup>e</sup>Nine cases rejected in one run.

<sup>f</sup>Ten cases rejected in one run.

Table II: Intercomparison between alpha-decay half-life-values calculated from the present Gamow-like model with and without product nucleus deformation included, and the experimental data for ground-state to ground-state alpha transitions of 174 even-even emitters ( $Q_2$  is the intrinsic electric quadrupole moment).

Parent nucleus		Product nucleus			Half life-values, $\tau$ (in second)		
$Z$	$A$	$Z_2$	$A_2$	$Q_2(b)$	Deformed product nucleus	Spherical product nucleus	Experimental
52	106	50	102	0.10	.540E-03	.518E-03	.600E-04
52	108	50	104	0.20	.181E+02	.171E+02	.430E+01
52	110	50	106	0.30	.512E+07	.473E+07	.620E+06
54	112	52	108	1.70	.212E+04	.192E+04	.320E+03
60	144	58	140	0.10	.311E+24	.268E+24	.720E+23
62	146	60	142	0.10	.784E+16	.702E+16	.320E+16
62	148	60	144	0.10	.760E+24	.655E+24	.220E+24
64	148	62	144	0.10	.514E+10	.472E+10	.230E+10
64	150	62	146	0.10	.138E+15	.125E+15	.560E+14
64	152	62	148	2.90	.106E+23	.867E+22	.340E+22
66	150	64	146	0.00	.208E+04	.208E+04	.120E+04
66	152	64	148	0.00	.206E+08	.206E+08	.860E+07
66	154	64	150	3.10	.136E+15	.115E+15	.950E+14

Parent nucleus		Product nucleus			Half life-values, $\tau$ (in second)		
$Z$	$A$	$Z_2$	$A_2$	$Q_2(b)$	Deformed product nucleus	Spherical product nucleus	Experimental
68	152	66	148	0.00	.200E+02	.200E+02	.110E+02
68	154	66	150	0.00	.671E+05	.671E+05	.480E+05
68	156	66	152	3.10	.704E+11	.606E+11	.230E+11
70	154	68	150	-0.20	.773E+00	.735E+00	.440E+00
70	156	68	152	-0.34	.946E+03	.890E+03	.260E+03
70	158	68	154	3.00	.462E+07	.408E+07	.430E+07
72	156	70	152	0.00	.314E-01	.314E-01	.250E-01
72	158	70	154	-0.40	.118E+02	.112E+02	.650E+01
72	160	70	156	2.80	.293E+04	.265E+04	.190E+04
72	162	70	158	3.80	.163E+07	.142E+07	.490E+06
72	174	70	170	7.00	.137E+25	.956E+24	.630E+23
74	158	72	154	0.30	.238E-02	.228E-02	.900E-03
74	160	72	156	0.90	.162E+00	.154E+00	.100E+00
74	162	72	158	2.50	.639E+01	.589E+01	.300E+01
74	164	72	160	3.50	.385E+03	.343E+03	.250E+03
74	166	72	162	4.10	.496E+05	.430E+05	.470E+05
74	168	72	164	4.80	.502E+07	.420E+07	.160E+07
76	162	74	158	0.70	.335E-02	.320E-02	.190E-02
76	164	74	160	2.20	.356E-01	.333E-01	.420E-01
76	166	74	162	3.20	.605E+00	.551E+00	.270E+00

Parent		Product			Half life-values, $\tau$ (in second)		
nucleus		nucleus			Deformed	Spherical	Experimental
$Z$	$A$	$Z_2$	$A_2$	$Q_2(b)$	product nucleus	product nucleus	
76	168	74	164	3.80	.101E+02	.904E+01	.450E+01
76	170	74	166	4.30	.166E+03	.145E+03	.610E+02
76	172	74	168	5.10	.489E+04	.412E+04	.960E+04
76	174	74	170	5.50	.324E+06	.267E+06	.220E+06
76	186	74	182	6.40	.395E+23	.291E+23	.630E+23
78	166	76	162	1.30	.541E-03	.516E-03	.300E-03
78	170	76	166	3.40	.304E-01	.278E-01	.600E-02
78	172	76	168	4.00	.204E+00	.182E+00	.110E+00
78	174	76	170	4.20	.220E+01	.195E+01	.110E+01
78	176	76	172	4.70	.335E+02	.291E+02	.170E+02
78	178	76	174	5.50	.761E+03	.638E+03	.270E+03
78	180	76	176	6.00	.225E+05	.184E+05	.170E+05
78	184	76	180	5.90	.103E+09	.835E+08	.100E+09
78	186	76	182	6.00	.666E+10	.533E+10	.530E+10
78	188	76	184	5.70	.122E+13	.984E+12	.340E+13
78	190	76	186	5.60	.929E+19	.728E+19	.100E+20
80	174	78	170	2.70	.122E-01	.114E-01	.210E-02
80	176	78	172	3.30	.279E-01	.256E-01	.340E-01
80	178	78	174	3.90	.429E+00	.386E+00	.360E+00
80	180	78	176	4.30	.625E+01	.554E+01	.610E+01
80	182	78	178	6.10	.785E+02	.650E+02	.710E+02
80	184	78	180	6.90	.216E+04	.172E+04	.280E+04

Parent nucleus		Product nucleus			Half life-values, $\tau$ (in second)		
$Z$	$A$	$Z_2$	$A_2$	$Q_2(b)$	Deformed product nucleus	Spherical product nucleus	Experimental
80	186	78	182	6.60	.388E+06	.311E+06	.410E+06
80	188	78	184	6.40	.236E+09	.188E+09	.530E+09
80	190	78	186	5.90	.547E+14	.435E+14	>.240E+10
82	180	80	176	-2.60	.268E-01	.249E-01	.400E-02
82	182	80	178	-2.80	.432E-01	.399E-01	.550E-01
82	184	80	180	-3.10	.445E+00	.406E+00	.550E+00
82	186	80	182	-3.20	.539E+01	.489E+01	.100E+02
82	188	80	184	-3.40	.141E+03	.127E+03	.110E+03
82	190	80	186	-3.40	.100E+05	.896E+04	.800E+04
82	192	80	188	-3.30	.258E+07	.229E+07	.370E+07
82	194	80	190	-3.30	.155E+10	.136E+10	.990E+10
82	196	80	192	-3.30	.485E+13	.421E+13	$\geq$ .740E+10
82	202	80	198	-3.10	.193E+31	.156E+31	>.170E+15
82	210	80	206	-0.20	.804E+16	.724E+16	.370E+17
84	190	82	186	0.00	.264E-02	.264E-02	.240E-02
84	192	82	188	0.00	.244E-01	.244E-01	.340E-01
84	194	82	190	0.00	.272E+00	.272E+00	.390E+00
84	196	82	192	0.10	.459E+01	.437E+01	.590E+01
84	198	82	194	0.10	.105E+03	.998E+02	.180E+03
84	200	82	196	0.10	.233E+04	.220E+04	.620E+04
84	202	82	198	0.10	.485E+05	.455E+05	.140E+06
84	204	82	200	0.00	.465E+06	.465E+06	.190E+07

Parent		Product			Half life-values, $\tau$ (in second)		
nucleus		nucleus			Deformed	Spherical	Experimental
$Z$	$A$	$Z_2$	$A_2$	$Q_2(b)$	product nucleus	product nucleus	
84	206	82	202	0.20	.319E+07	.298E+07	.140E+08
84	208	82	204	-0.20	.119E+08	.111E+08	.910E+08
84	210	82	206	-0.20	.969E+06	.906E+06	.120E+08
84	212	82	208	0.00	.213E-06	.213E-06	.300E-06
84	214	82	210	0.00	.176E-03	.176E-03	.160E-03
84	216	82	212	0.00	.169E+00	.169E+00	.150E+00
84	218	82	214	0.20	.229E+03	.217E+03	.190E+03
86	196	84	192	-5.60	.155E-01	.131E-01	<.300E-02
86	200	84	196	0.50	.997E+00	.951E+00	.110E+01
86	202	84	198	0.40	.897E+01	.853E+01	.110E+02
86	204	84	200	0.40	.661E+02	.627E+02	.100E+03
86	206	84	202	0.40	.269E+03	.255E+03	.550E+03
86	208	84	204	0.30	.811E+03	.767E+03	.240E+04
86	210	84	206	-0.50	.209E+04	.197E+04	.900E+04
86	212	84	208	-0.50	.200E+03	.189E+03	.140E+04
86	214	84	210	0.10	.247E-06	.240E-06	.270E-06
86	216	84	212	0.00	.840E-04	.840E-04	.450E-04
86	218	84	214	-0.23	.646E-01	.617E-01	.350E-01
86	220	84	216	0.60	.104E+03	.984E+02	.560E+02
86	222	84	218	1.10	.578E+06	.540E+06	.330E+06
88	202	86	198	-6.00	.359E-02	.300E-02	.700E-03
88	204	86	200	-5.70	.602E-01	.509E-01	.590E-01
88	206	86	202	-3.00	.265E+00	.244E+00	.240E+00

Parent		Product			Half life-values, $\tau$ (in second)		
nucleus		nucleus			Deformed	Spherical	Experimental
$Z$	$A$	$Z_2$	$A_2$	$Q_2(b)$	product nucleus	product nucleus	
88	208	86	204	-2.50	.771E+00	.718E+00	.140E+01
88	210	86	206	-1.50	.155E+01	.147E+01	.380E+01
88	212	86	208	-0.90	.436E+01	.414E+01	.140E+02
88	214	86	210	-0.80	.525E+00	.499E+00	.250E+01
88	216	86	212	0.00	.200E-06	.200E-06	.180E-06
88	218	86	214	0.20	.498E-04	.480E-04	.260E-04
88	220	86	216	0.20	.306E-01	.293E-01	.180E-01
88	222	86	218	1.10	.587E+02	.556E+02	.390E+02
88	224	86	220	3.50	.536E+06	.484E+06	.330E+06
88	226	86	222	4.40	.921E+11	.799E+11	.530E+11
90	210	88	206	-4.30	.125E-01	.112E-01	.900E-02
90	212	88	208	-3.30	.220E-01	.203E-01	.300E-01
90	214	88	210	-1.70	.505E-01	.478E-01	.100E+00
90	216	88	212	-1.10	.758E-02	.724E-02	.280E-01
90	218	88	214	0.20	.167E-06	.162E-06	.110E-06
90	220	88	216	0.20	.205E-04	.198E-04	.970E-05
90	222	88	218	0.50	.365E-02	.351E-02	.280E-02
90	224	88	220	3.20	.172E+01	.159E+01	.130E+01
90	226	88	222	4.20	.359E+04	.323E+04	.240E+04
90	228	88	224	5.80	.126E+09	.107E+09	.830E+08
90	230	88	226	6.30	.509E+13	.418E+13	.310E+13
90	232	88	228	6.80	.108E+19	.857E+18	.570E+18
92	218	90	214	-1.60	.349E-03	.333E-03	.150E-02

Parent nucleus		Product nucleus			Half life-values, $\tau$ (in second)		
$Z$	$A$	$Z_2$	$A_2$	$Q_2(b)$	Deformed product nucleus	Spherical product nucleus	Experimental
92	222	90	218	0.20	.415E-05	.402E-05	.100E-05
92	224	90	220	1.00	.705E-03	.676E-03	.900E-03
92	226	90	222	4.20	.405E+00	.369E+00	.200E+00
92	228	90	224	5.80	.900E+03	.782E+03	<.570E+03
92	230	90	226	6.70	.384E+07	.320E+07	.270E+07
92	232	90	228	7.20	.460E+10	.373E+10	.320E+10
92	234	90	230	7.80	.141E+14	.110E+14	.110E+14
92	236	90	232	8.20	.153E+16	.118E+16	.100E+16
92	238	90	234	8.30	.355E+18	.269E+18	.180E+18
94	228	92	224	5.70	.380E+00	.336E+00	.200E+00
94	230	92	226	6.60	.196E+03	.168E+03	$\geq$ .200E+03
94	232	92	228	7.20	.137E+05	.114E+05	.160E+05
94	234	92	230	8.10	.846E+06	.682E+06	.530E+06
94	236	92	232	8.50	.124E+09	.980E+08	.130E+09
94	238	92	234	8.80	.354E+10	.275E+10	.390E+10
94	240	92	236	9.00	.327E+12	.251E+12	.280E+12
94	242	92	238	9.10	.175E+14	.133E+14	.150E+14
94	244	92	240	8.70	.289E+16	.220E+16	.320E+16
96	238	94	234	8.50	.230E+06	.185E+06	$\geq$ .860E+05
96	240	94	236	8.50	.215E+07	.172E+07	.330E+07
96	242	94	238	9.30	.148E+08	.115E+08	.190E+08
96	244	94	240	9.60	.546E+09	.418E+09	.750E+09

Parent nucleus		Product nucleus			Half life-values, $\tau$ (in second)		
$Z$	$A$	$Z_2$	$A_2$	$Q_2(b)$	Deformed product nucleus	Spherical product nucleus	Experimental
96	246	94	242	9.70	.131E+12	.991E+11	.180E+12
96	248	94	244	9.70	.110E+14	.822E+13	.140E+14
96	250	94	246	9.40	.856E+13	.648E+13	.280E+13
98	240	96	236	8.80	.578E+02	.470E+02	.640E+02
98	242	96	238	8.90	.279E+03	.226E+03	.260E+03
98	244	96	240	9.10	.143E+04	.114E+04	.150E+04
98	246	96	242	9.20	.107E+06	.845E+05	.160E+06
98	248	96	244	10.20	.196E+08	.149E+08	.350E+08
98	250	96	246	10.30	.260E+09	.196E+09	.490E+09
98	252	96	248	10.30	.816E+08	.616E+08	.100E+09
98	254	96	250	9.40	.232E+10	.180E+10	.200E+10
98	256	96	252	9.20	.279E+12	.216E+12	.740E+11
100	246	98	242	9.40	.183E+01	.148E+01	.120E+01
100	248	98	244	9.90	.272E+02	.216E+02	.450E+02
100	250	98	246	9.80	.102E+04	.803E+03	<200E+04
100	252	98	248	9.90	.359E+05	.281E+05	.110E+06
100	254	98	250	10.80	.795E+04	.605E+04	.140E+05
100	256	98	252	10.70	.101E+06	.768E+05	.140E+06
102	250	100	246	10.00	.130E+00	.105E+00	.500E+00
102	252	100	248	10.20	.207E+01	.165E+01	.420E+01
102	254	100	250	10.20	.220E+02	.174E+02	.720E+02

Parent nucleus		Product nucleus			Half life-values, $\tau$ (in second)		
$Z$	$A$	$Z_2$	$A_2$	$Q_2(b)$	Deformed product nucleus	Spherical product nucleus	Experimental
102	256	100	252	10.50	.134E+01	.106E+01	.360E+01
102	258	100	254	10.10	.328E+02	.260E+02	.120E+03
104	254	102	250	10.30	.335E-01	.269E-01	.170E+00
104	256	102	252	10.30	.540E+00	.432E+00	.360E+00
104	258	102	254	10.80	.398E-01	.315E-01	.110E+00
104	260	102	256	10.40	.649E+00	.518E+00	.100E+01
106	260	104	256	11.10	.406E-02	.322E-02	.850E-02
108	264	106	260	11.00	.352E-03	.284E-03	.100E-03

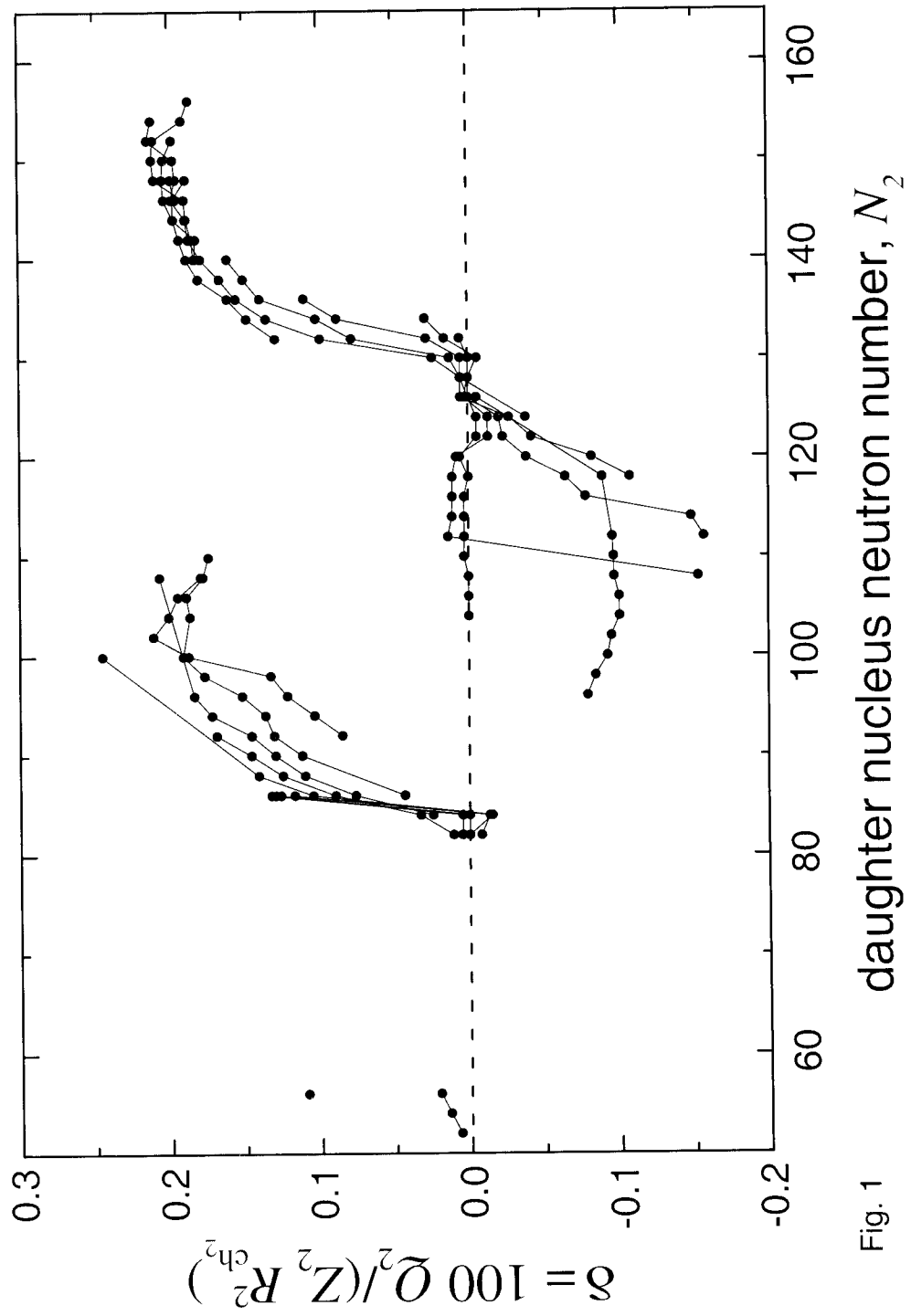


Fig. 1

daughter nucleus neutron number,  $N_2$

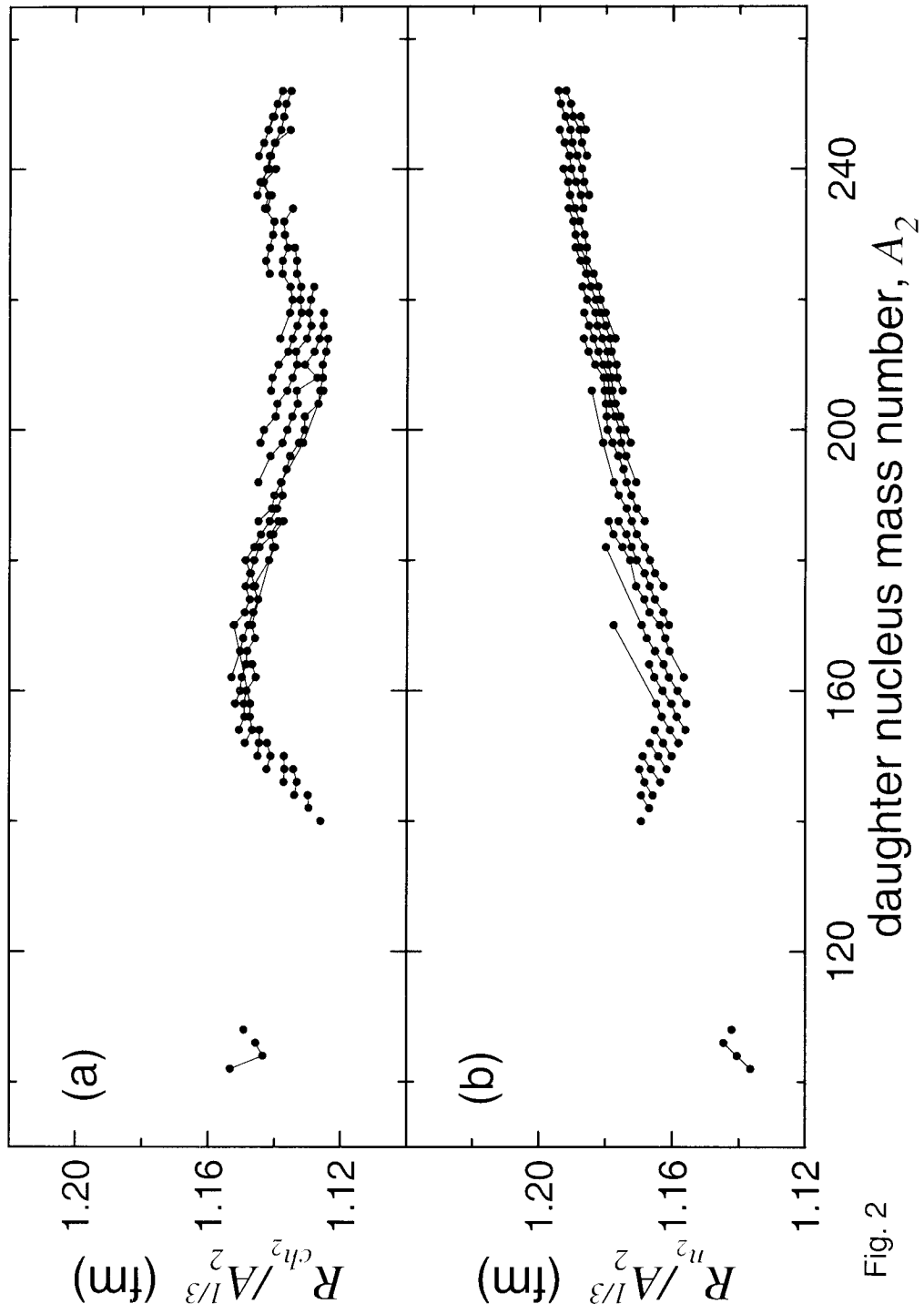


Fig. 2

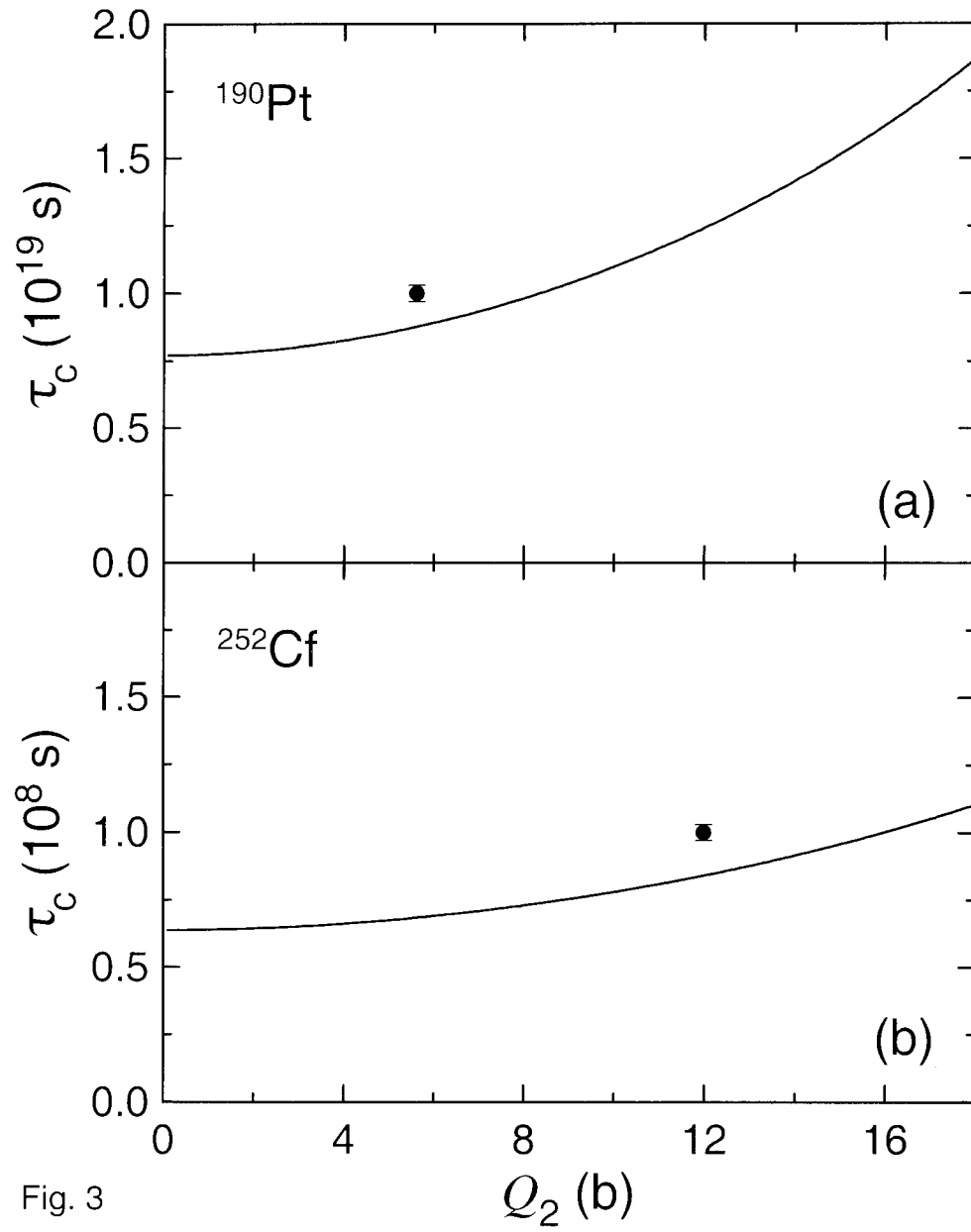


Fig. 3

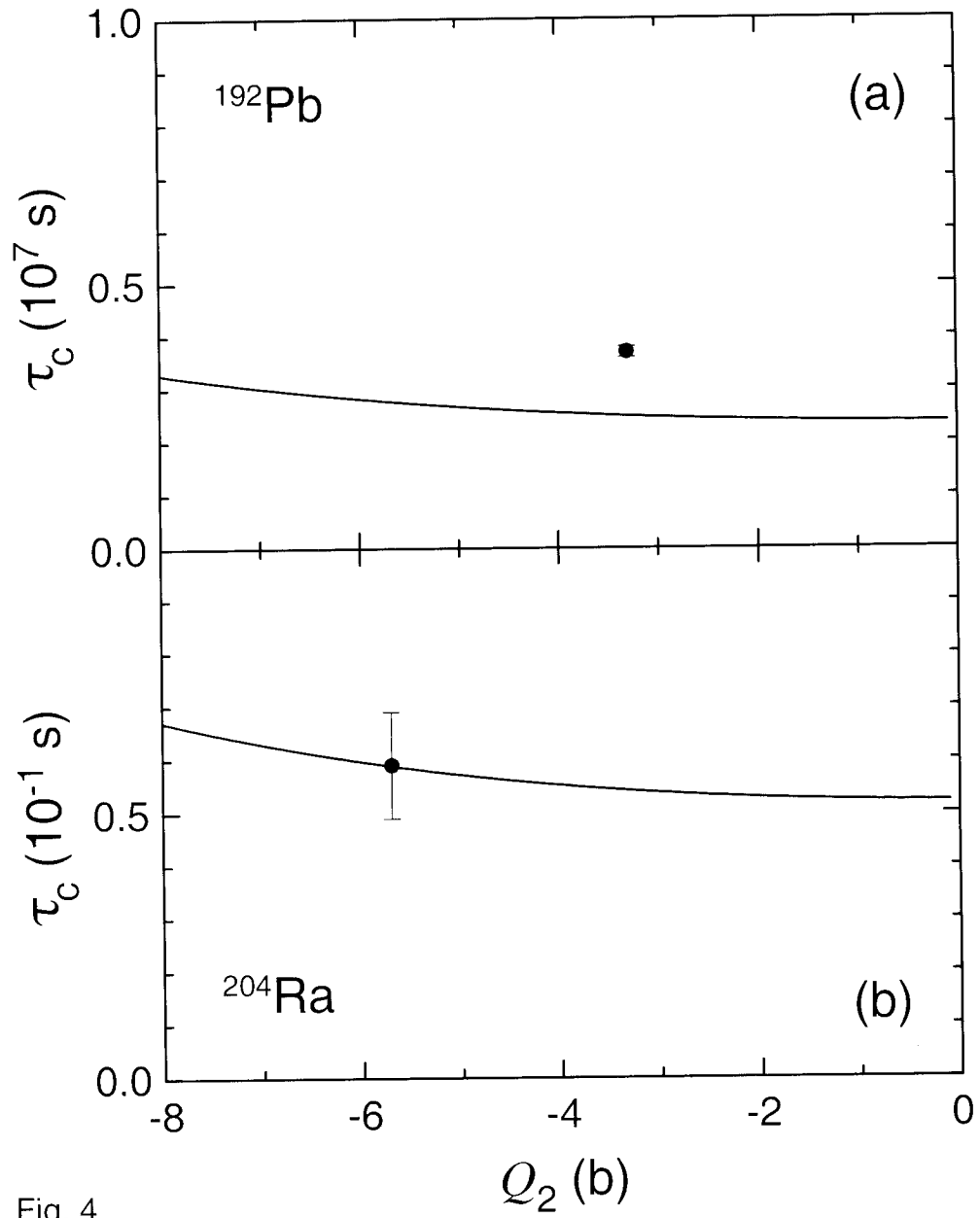
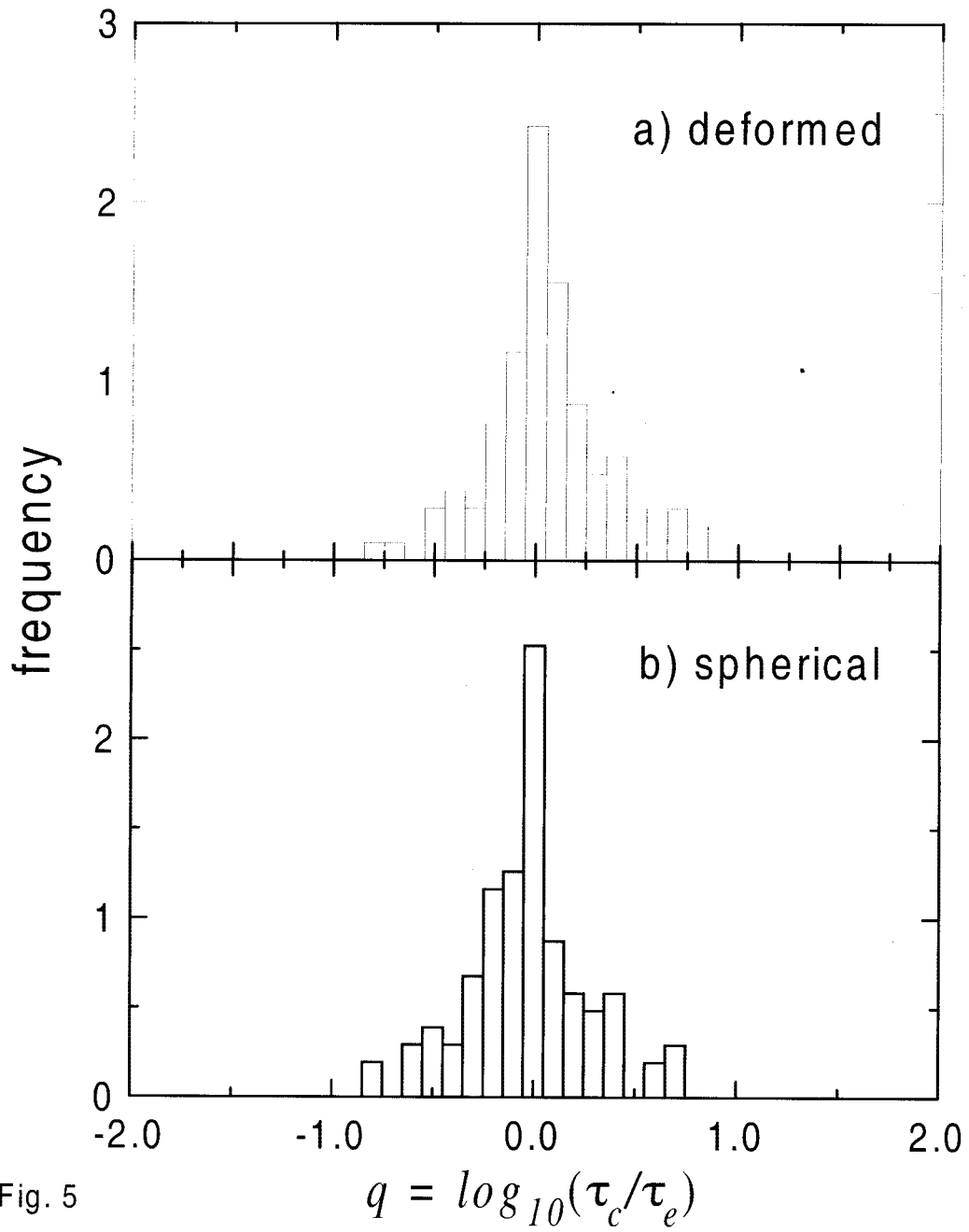


Fig. 4



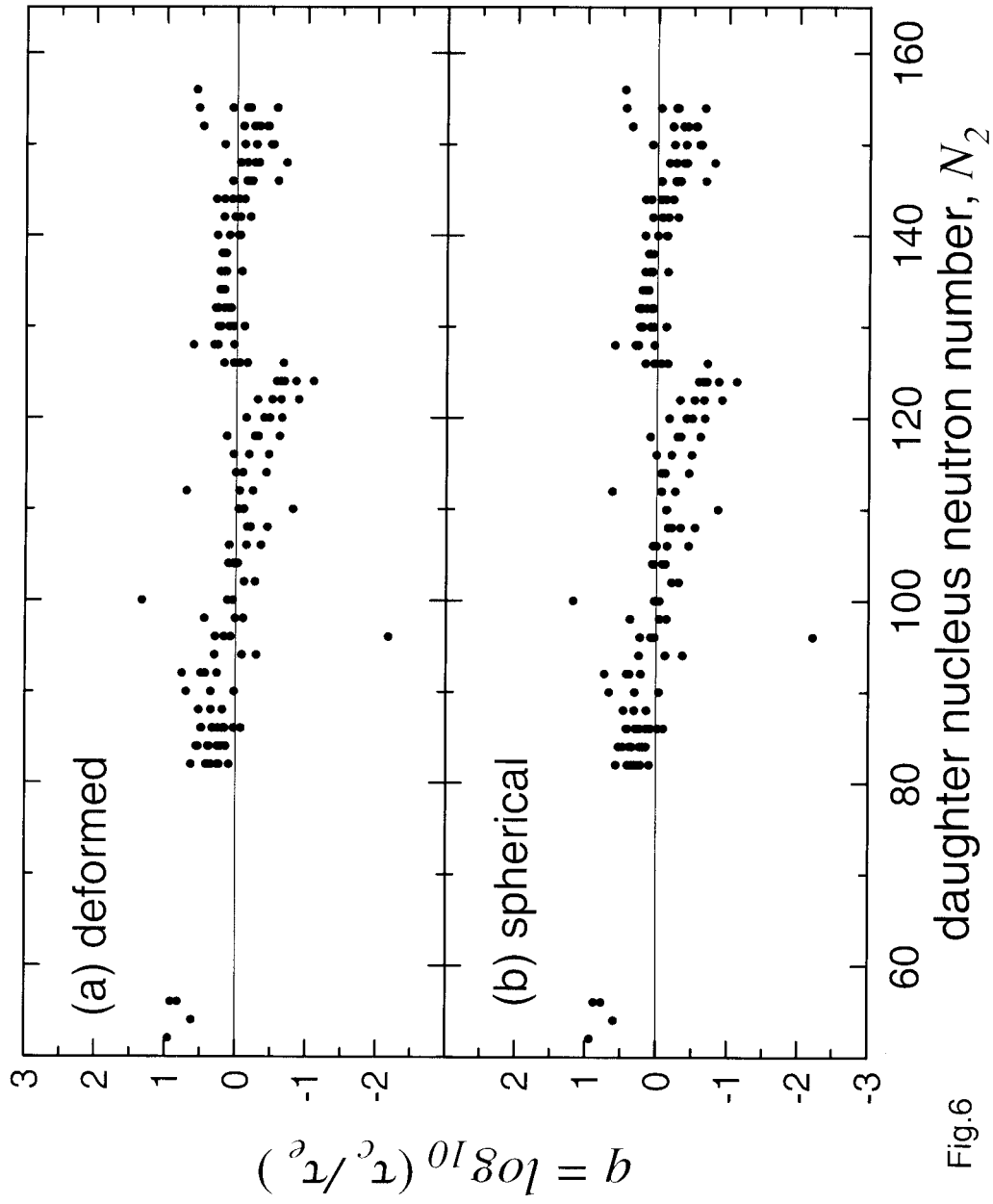


Fig.6